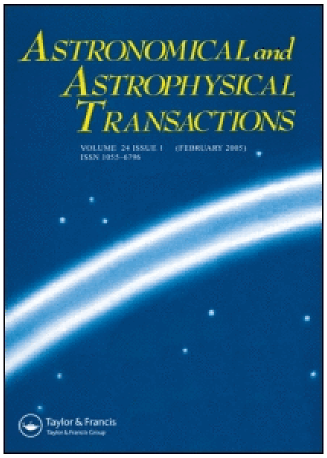

Astronomical & Astrophysical Transactions
The Journal of the Eurasian Astronomical Society
Publication details, including instructions for authors and subscription information:
http://www.informaworld.com/smpp/title~content=t713453505

ON the origin of solar filament magnetic fields

V. M. Grigoryev [a]; L. V. Ermakova [a]
[a] Institute of Solar-Terrestrial Physics RAS, Irkutsk 33, Russia

Online Publication Date: 01 January 1999
To cite this Article: Grigoryev, V. M. and Ermakova, L. V. (1999) 'ON the origin of solar filament magnetic fields', Astronomical & Astrophysical Transactions, 17:5, 355 - 365
To link to this article: DOI: 10.1080/10556799908244085
URL: http://dx.doi.org/10.1080/10556799908244085

Astronomical and Astrophysical Transactions, 1999,
Vol. 17, pp. 355–365
Reprints available directly from the publisher
Photocopying permitted by license only

ON THE ORIGIN OF SOLAR FILAMENT MAGNETIC FIELDS

V. M. GRIGORYEV and L. V. ERMAKOVA

Institute of Solar-Terrestrial Physics RAS, P. O. Box 4026, Irkutsk 33, 664033, Russia

(Received May 23, 1997)

An analysis is made of vector-magnetograms and of the velocity network associated with supergranulation in the photosphere, in the region of a quiescent filament. Observational data were obtained with the Sayan observatory vector-magnetograph. It is shown that (1) near the filament the magnetic field tends to be directed along the filament, and (2) supergranules line up along the filament, with the formation of a nearly continuous line of supergranule boundaries. A prominence model is suggested, accounting for many observed properties obtained in recent years. It is a dynamic model where the magnetic field is the combination of the large-scale field and flux tubes continually emerging between supergranules in the region of the polarity inversion line of the large-scale magnetic field that are aligned along that line. The coherent properties of the emerging tubes and their orientation are associated with topological pumping of the subphotospheric magnetic field by supergranulation convection. The system of emerging magnetic tubes in the result of reconnection forms a horizontal magnetic field along the filament where a cold plasma from the photosphere and chromosphere penetrates.

KEY WORDS Magnetic fields, filament

1 INTRODUCTION

Many filaments show up as chains of loops whose ends (footpoints) cling to each other. The filament body, which composes the loop tops, resides in the corona, with its footpoints going down into the chromosphere. The penetration depth of the footpoints depends on the type of filaments; in some cases they can reach the photosphere. The chromospheric structure in the neighbourhood of filaments and the structure of the filaments themselves testify that the magnetic field plays the decisive role, and suggest some conclusions about the magnetic framework of the filaments (Foukal, 1971; Martin, Bilimora and Tracadas, 1994). By analysing the distances between filament footpoints, it was anticipated that they are anchored in interspaces between supergranules (Sykora, 1968). The presence of a connection between the filament magnetic structure and convection places certain requirements upon models for filament formation. Plocienia and Rompolt (1973) determined the position of 320 footpoints for 100 filaments with respect to chromospheric network cells on K Ca II-filtergrams portraying the supergranule pattern, and arrived at the conclusion that in 90% of cases they are confidently associated with cell boundaries. However, the above-mentioned research does not answer the question: Do the filaments lie largely above supergranule boundaries or can they traverse supergranule cells resting with their footpoints on areas between them? Kartashova (1979), by studying filtergrams in the H-alpha core and wings, concluded that diffuse filaments are located over chromospheric network cell boundaries, while filaments in flocculi are aligned independently of them. A total of 20 filaments were examined. Unfortunately, the author did not specify which objects were observed. Two filaments in flocculi, cited as an example, were not stable, their lengths changed from day to day, some parts disappeared, and some new parts appeared. The presentation of material includes some contradictions. Furthermore, using indirect information always implies some arbitrariness. From what has been said it appears reasonable to conclude that there is no convincing evidence for the independence of the location of stable filaments, unassociated with active regions, with respect to supergranule network cells. No attempt was made to determine the picture of supergranule arrangement in the neighbourhood of filaments by analysing the recorded line-of-sight velocity fields. Usually, such observations are made to objects located near the disk centre (see, for example, Ioshpa and Kulikova, 1995) where the contribution from supergranule motion is very small and unidentifiable.

Filaments lie over magnetic field polarity inversion lines. This is the starting factor when constructing models. At the same time, direct measurements of the transversal magnetic field are not so numerous. We did not find any reports on the analysis of the transversal magnetic field pattern in the region of quiescent filaments. When developing models for filament formation, it is customary to make some assumptions, sometimes strengthened by indirect data on the transversal magnetic field structure. It is known that near a filament H-alpha fibrilles are arranged along it (Foukal, 1971). However, although the direction of fibrilles generally reflects the direction of magnetic field lines (Tsap, 1964), it is beyond reason to extend this directly to a rather limited photospheric area under the filament.

The goal of this paper is to analyse some observational data concerning the supergranulation convection structure and the transversal component of the magnetic field in the photosphere in the vicinity of a filament. Next we discuss qualitatively the possible models and suggest a model based on the stochastic origin of the fine structure of chromospheric filaments and the determinate origin of large-scale properties of the polarity inversion line, where the filament forms.

2 DATA

Observational data from the Sayan observatory vector-magnetograph (Grigoryev, 1985) and H-alpha filtergrams from the Baikal observatory obtained in the core and the blue wing, are used in this study. In our detailed analysis, we used a fragment of the magnetogram and the line-of-sight velocity map for August 23, 1989, of size 312 × 304 arcsec which contains the filament and the following sunspot of the active region Mt. Wilson 25464. The location of the centre of the chosen area was W33N28. Within this area of the solar surface the pixel size ranges from 6000 to 8000 km. The instrument's sensitivity to the longitudinal and transversal magnetic fields and to line-of-sight velocities is, respectively, 1 G, 80 G, and 100 m s^{-1}. The uncertainty in the superposition of the H-alpha images and vector-magnetograph maps was 4 arcsec. Line-of-sight velocities were corrected for solar rotation.

The filament was formed on the invisible solar hemisphere and appeared from behind the limb on August 14. Comparison of H-alpha filtegrams with Stanford large-scale magnetic field maps shows that the filament lies along magnetic field cell boundaries, with its central part and ends being directed along the meridian and the equator, respectively. Eastward of it lies the active region Mt. Wilson 25469, and an extended complex, consisting of the active regions 25463, 25465 and 25464, is to the west. Throughout its disk passage, the filament underwent no dramatic changes. By August 23, the filament decreased in length because of the disappearance of portions directed along the equator, which is consistent with changes in the large-scale pattern of the magnetic field. At that time the filament was 20 degrees in length, and the filament was discontinuous near its southern end. When examining the filament at different viewing angles and assuming a relative invariability of the object, it can be concluded that the filament shows up as a dense wall 16 000–18 000 km in height and no less than 2000 km in thickness, and its slope to the solar surface varies along the length.

3 RESULTS

3.1 The Arrangement Pattern of Supergranules

According to Rimmele and Schroter (1989), supergranules in the latitude range under consideration are 33 000–35 000 km in diameter. It approximates 4–5 pixels depending on the distance from the disk centre. The rate at which material spreads in supergranules averages 450 m s^{-1}, which, when projected onto the line of sight, gives 200–370 m s^{-1} depending on whether these portions lie nearer to the solar disk centre or farther from it.

The residual contributions of non-supergranulation motions in recorded line-of-sight velocities does not exceed 215 m s^{-1} (see Appendix). Notwithstanding the fact that we are dealing with overvalued velocities, it is clearly unlikely that the arrangement pattern of supergranules can be reconstructed simply by analysing the line-of-sight velocity map. Only single supergranules can be identified with such a procedure.

In solving the formulated problem, we applied the digital non-recursive filter. The performance of the filter is described by the formula

$$y_{ij} = \sum_{k=-2}^{k=2} c_k V_{i-k,j},$$

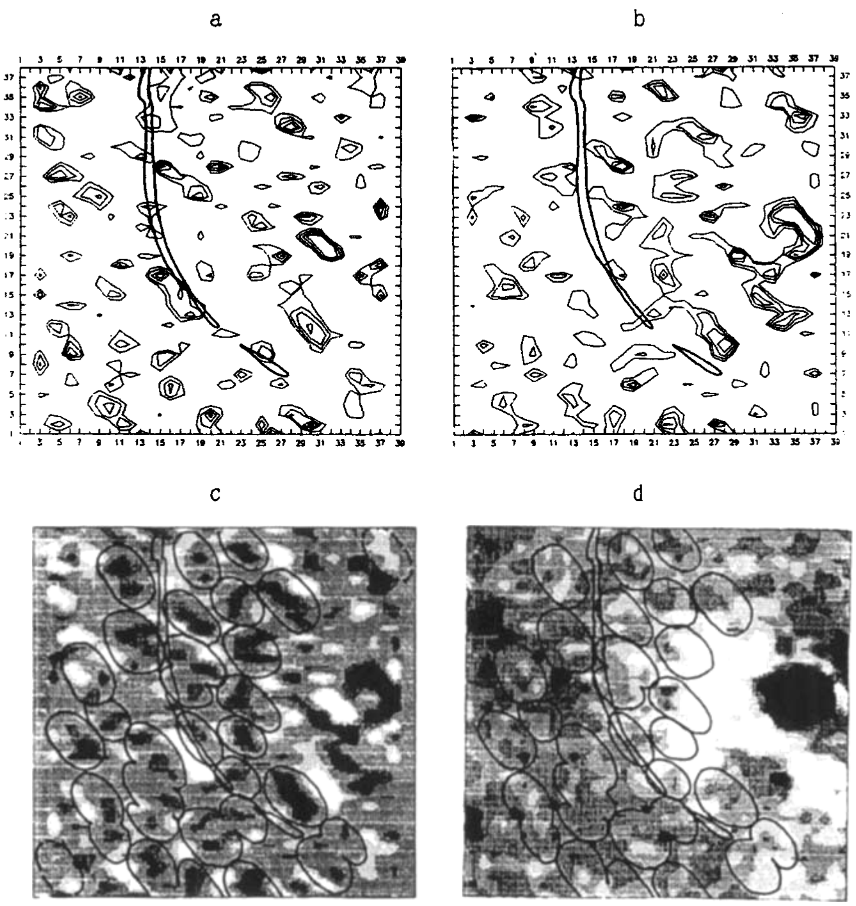

Figure 1 The supergranule network in the filament neighbourhood. Here are contour distribution maps for negative (a) and positive (b) values of the function y_{ij}, and the supergranule arrangement pattern superimposed on the field y_{ij} (c) and on the longitudional magnetic field (d). The average supergranules sizes are shown with dotted contours in the bottom left and in the top right (c). The filament contour is drawn N–E orientation is usual.

where $V_{i-k,j}$ is the line-of-sight velocity at a point with coordinates $(i-k, j)$, c_k stands for filter constants, and y_{ij} is the output signal for a point with coordinates i, j. Since, on the one hand, the measured quantity and the error of measurement are intercomparable and, on the other, the supergranule cross-section accommodates no more than 2–3 resolution elements with the line-of-sight velocity of the same sign, it would serve no purpose to take into account the true velocity distribution across a supergranule. Therefore, the filter with constant $c_k = 1, 1, 0, -1, -1$ was used. After applying such a filter, lines of a change of sign of the line-of-sight velocity corresponding to cell boundaries and centres, respectively, will be represented by negative and positive values, provided that the cell size is no less than 4 pixels. The filter noise is 2.

Figures 1(a) and (b) show contour distribution maps for negative and positive values of the function y_{ij}, respectively, with isolines ± 3, 6, 9, 12. Figures 1(c) and (d) portray the supergranule arrangement pattern superimposed, in the former case, on the field y_{ij} and, in the latter, on the longitudinal magnetic field. The northern end of the filament 15 arcsec in extent is outside the observed zone. One can see that predominantly negative rather than positive values of y_{ij} are beneath the filament. Whenever the filament falls within the region of positive values, they do not reach the level of the second contour. Consequently, our filtering shows that the filament location is correlated with lines of change of sign of the line-of-sight velocities corresponding to supergranule boundaries. Figure 1 shows the possible supergranule network for this pattern. Some cells are not fully spatially resolved. There is a reasonably good agreement with the expected supergranule size. Figure 1(d) shows a map for the longitudinal magnetic field with a superposed supergranule network. In the majority of cases, at the centre of the deduced convective cell the longitudinal magnetic field is weaker compared to the edges. This is characteristic for supergranules. Hence our analysis counts in favour of the fact that the filament being investigated lies over supergranule boundaries.

3.2 Orientation of the Transversal Magnetic Field with Respect to the Filament

Figure 2 shows a map for transversal magnetic field azimuths where in the neighbourhood of the filament a discontinuous line is shown, which separates regions with the transversal magnetic field directed along and across the filament. The data apply to $H_{\mathrm{tr}} \geq 80$ G.

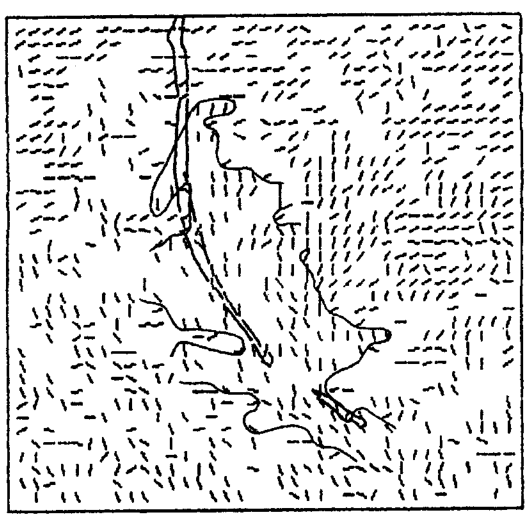

Figure 2 The transversal magnetic field azimuths. A discontinuous line separates regions with the transversal magnetic field directed along and across the filament. The filament contour is drawn.

One can see that, westward of the filament in the immediate neighbourhood of it, the transversal field is directed along the filament, and only near the northern end has it an approximately normal direction. This is compatible with the overall pattern of transversal magnetic field orientation in this region which is determined by the powerful active region Mt. Wilson 25464. Eastward of the filament, the magnetic field is weaker and fragmented and shows up as a conglomerate of modest-sized systems. In this case the transversal field reverses its direction on relatively small scales. Nevertheless, along a significant filament length, zones with the transversal field directed along the filament are adjacent to it. Hence it can be concluded that along most of the length of the filament in its photospheric neighbourhood and immediately beneath it, the transversal magnetic field is oriented along the filament.

4 ON THE FILAMENT MAGNETIC FIELD MODEL

The main parameters and properties of solar filaments and prominences are well established. A theoretical treatment of filaments was generally restricted to two-dimensional models, such as those due to Kippenhahn and Schluter (1957), and Kuperus and Raadu (1974). The main difference between them is how the filament magnetic field is correlated with the surrounding photospheric magnetic fields and how it determines the two orientations of the field called "normal" and "inverse" (Priest *et al.*, 1989). Such models were considered in greater detail by Hirayama (1985), Anzer (1984), Van Ballegooijen and Martens (1989, 1990), Demoulin and Priest (1993), Hundhausen and Low (1994), and Cartledge and Priest (1994). These models ignored the axial magnetic field along the filament, with its direction opposite to that expected from the action of differential rotation on the originally potential coronal magnetic arcades.

Models based on longitudinal twisted magnetic field tubes were recently considered by Priest, Hood and Anzer (1989), Hood and Priest (1979), Low (1993), and Rust and Kumar (1994). More recently, there appeared a pioneering paper of Martin, Bilimoria and Tracadas (1994) which strongly suggests that conventional approaches to the filament problem should be revised. Martin and Echols (1994) put forward a qualitative model for prominence structure. The most adequate attempt at constructing a quiescent filament model, in agreement with the observations by Martin *et al.* (1994), was made by Rust and Kumar (1994), and Priest *et al.* (1996). All models intend to explain the filament structure on a deterministic basis alone.

We have tried to construct a qualitative model for quiescent filaments, based on the global large-scale structure of the magnetic field and the coherent organization of the fine structure of the chromosphere of a stochastic nature.

Qualitatively, the magnetic field structure in the filament is shown in Figure 3. The filament lies above the separation line of opposite-polarity large-scale magnetic field regions observed in the photosphere. The coronal field is a nearly potential field and appears as arcades connecting opposite-polarity regions. The field structure in subphotospheric layers is unknown, but some relevant guesses will be discussed in

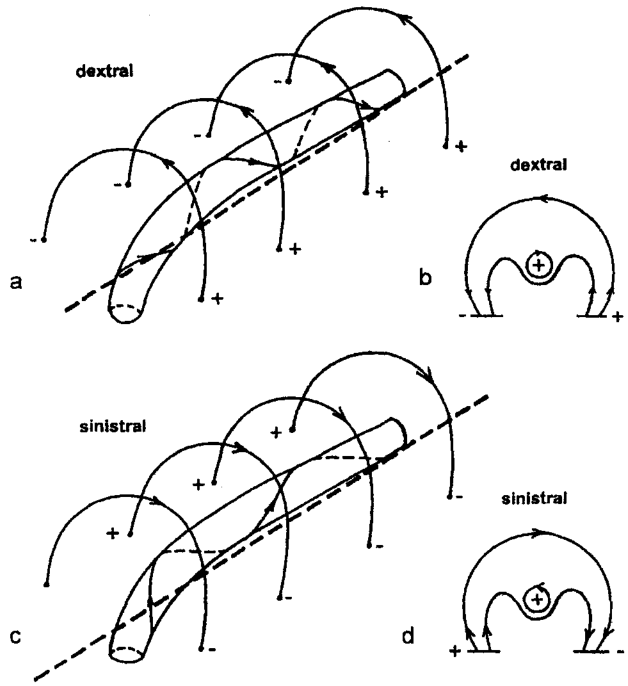

Figure 3 The filament magnetic field structure. The azimuthal component of filament magnetic field directed opposite to the magnetic field of the coronal arcade has a right-handed helical structure for dextral filaments (*a*, *b*) and a left-handed one for sinistral filaments (*c*, *d*).

what follows. Further, we surmise that, in the region of the polarity inversion line, magnetic flux tubes are continually emerging to produce an axial magnetic field in the filament. The axial magnetic field beneath the arches affords stability to the entire system because it produces shear, i.e., arches of different heights lying beneath each other and slightly swung with respect to each other. In addition, if emerging magnetic flux tubes are twisted in such a manner that the azimuthal component of the field in the upper part of the filament has a direction opposite to that of the field at the top of the coronal arcade (Figures 3(*b*) and (*d*)), then the reconnection will result in a deflection at the top of arches. This deflection of coronal arches ensures filament stability.

Thus, the model assumes three necessary conditions for filament formation:

(1) There exists a system of magnetic arches in the corona which is associated with the large-scale magnetic field in the photosphere.

(2) The axial magnetic field beneath coronal arches is produced by continually emerging magnetic tubes oriented along the polarity inversion line.

(3) Twisted flux tubes, as they emerge from the photospere, have the azimuthal component of field opposite to the field direction at the top of coronal arcades.

These three necessary conditions can be realized only by the two magnetic field structures shown in Figures 3(a) and (c). If, for example, the twisting is changed from right-hand to left-hand or if the axial field direction is reversed, then the field structure does not produce a deflection of arches and no filament stability is ensured. As is evident from Figures 3(a) and (c), these two field structures correspond to two classes of magnetic configurations discovered by Martin, Bilimoria and Tracadas (1994). Figure 3(a) corresponds to a dextral filament with right-bearing fine structure in the filament, and Figure 3(c) corresponds to the sinistral type with left-bearing fine structure. How is the axial magnetic field produced in the filament? Both a determinate and stochastic mechanism can be at work in this case.

Priest *et al.* (1996) speculated that the toroidal magnetic field that is produced by differential rotation beneath the solar surface can be brought to the surface by magnetic buoyancy and can give loops oriented along the polarity inversion line. However, such a supposition would not do for quiescent filaments lying in middle and low latitudes on the boundary of large-scale bipolar magnetic regions and oriented at a large angle to the solar equator (sometimes elongated in a meridional direction).

We suggest one further possible formative scenario for the filament axial magnetic field connected with the magnetic field structure in supergranule convection.

Quiescent filaments are typically located on the polarity inversion line of large-scale magnetic fields. The large-scale magnetic field is the result of the active region magnetic field evolution. Not only does the magnetic flux diffuse, after the active region decays, but some part of it submerges below the photosphere. The diffuse magnetic flux is controlled by supergranule convection (Garcia de la Rosa, 1983). Drobyshevski and Yuferev (1974) and Arter *et al.* (1983) showed that the topology of supergranulation cells pumps weak magnetic fields into the cell bottom (topological pumping) to form a magnetic sheet there. This process is based on the connection between the structure of the downflow and the isolated structure of the upflow of material. Weak magnetic fields are displaced to the periphery of the cells and come down. The continuous horizontal magnetic flux is conserved at the cell bottom, and if the flux concentration reaches a critical value, it can emerge under the action of magnetic buoyancy forces along the cell boundaries, going from one cell to another. Schematically, this is shown in Figure 4. The direction of these horizontal magnetic fields at the cell bottom must conserve the mean direction of the subphotospheric connection of two parts, the bipolar magnetic region. Conceivably there is a tendency for this horizontal field to reverse along the polarity inversion line due to the meridional drift of the leading part equatorward and of the following part poleward, as well as because the field is expelled into the polarity inversion region where the vertical magnetic field is very weak or absent. There is no conclusive answer lo this question yet, but our reported observations, combined with observations of the transversal field on the polarity inversion line in the active region (Gary *et al.*, 1987; Gary and Hagyard, 1990) show that the transversal component of the mag-

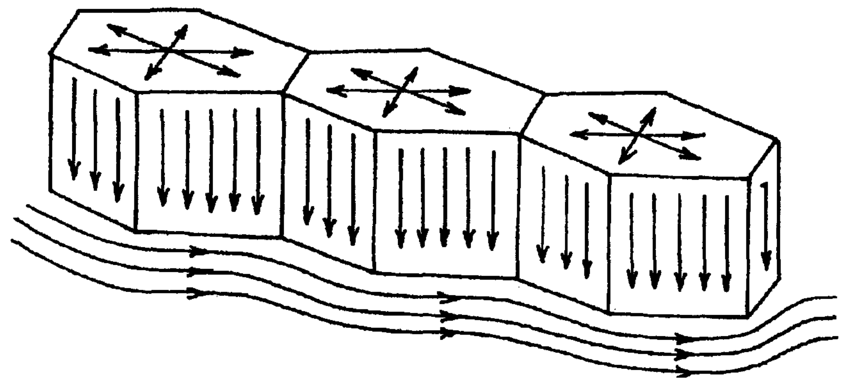

Figure 4 The continuous horizontal magnetic field is accumulated at the supergranule bottom. If the magnetic flux concentration reaches a critical value, the magnetic field can emerge under the action of magnetic buoyancy forces along the convective cell boundaries, passing from one cell to another.

netic flux is directed along the polarity inversion line whenever a filament exists.

Finally, we propose a stochastic formative scenario for the axial field and the related twisting which would remove all difficulties when explaining the orientation of the subphotospheric horizontal field. It would appear reasonable that in the region of the polarity inversion line, as on the entire solar surface, magnetic flux tubes emerge and persist at the base of supergranulation cells due to topological pumping. In this case their orientation with respect to the polarity inversion line can be different (random). But only those flux tubes which have the orientation of the axial component and the twisting with respect to the polarity inversion line corresponding to the two situations shown in Figures 3(a) and (b) will be "captured" by coronal arcades and will conserve stability and form the structure of the filament as a large-scale entity. The other flux tubes will disappear because of instability or reconnection, as is the case in the other part of the solar surface. This can ensure the predominant twisting of the emerging magnetic flux ropes by Coriolis force acting on the emerging and expanding flux tubes. In the northern hemisphere, flux tubes are rotated clockwise, and in the southern hemisphere, the situation is the opposite. Thus, the large-scale structure of coronal arcades and the twisting of continually emerging flux tubes will choose, for the formation of a stable structure of the filament, only those flux tubes (fibrilles as elementary "building" elements) which do ensure the two stable filament configurations: dextral and sinistral (Figures 3(a) and (c)).

Acknowledgements

We wish to thank Dr. A. V. Mordvinov for assistance with computations. This work was done with the support of the Russian Foundation for Fundamental Research, grant 96–02–16647a and governmental support grant for leading scientific schools 96–15–96733.

Appendix. Estimation of the Residual Contributions of Non-Supergranulation Motions

In addition to instrumental noise, there are other factors which mask the pattern of super-granule motions.

After introducing a correction for solar rotation into recorded line-of-sight velocities, the remaining signal, in a general case, represents a superposition of velocities associated with convection, 5-minute oscillations, and with large-scale motions of a different nature.

Among different-scale convective structures, significant velocities are recorded, in addition to supergranules, in granules and mesogranules. In this particular case the first type must not make any marked contribution because the granule size is much smaller than the resolution element. The typical spatial scale of mesogranules is 5–7 arcsec (Brandt *et al.*, 1991), the vertical velocity is 60 m s^{-1}, and the mean horizontal velocity approachs that of supergranules (Title *et al.*, 1986, 1989; Brandt *et al.*, 1988), i.e., the line-of-sight velocity for the centre of the area on the solar surface under consideration averages 300 m s^{-1}. The height of the spectrograph entrance slit (8 arcsec) exceeds by a factor of 1.5–2 the mesogranule size; consequently, one resolution element can accommodate a non-compensated line-of-sight velocity of about 100 m s^{-1}.

The contribution from the 5-minute oscillations can be inferred based on results obtained by Kobanov (1985). The largest mean vertical velocity of 175 m s^{-1} is attained for the typical scale of 24 arcsec which is defined as the distance between the two nearest points on the solar surface oscillating with the same phase. When projected onto the line of sight, for the centre of the observed area this amounts to 120 m s^{-1}. Since the typical spatial scale in this case exceeds the spatial resolution of the observation, this value can be thought of as the upper limit of the mean value of the line-of-sight velocity caused by the 5-minute osculations. It should be noted that, according to Malherbe *et al.* (1981), the 5-minute oscillations of the photosphere beneath the filament are significantly weaker.

High-precision measurements carried out by Ioshpa and Kulikova (1995) may be used for taking into account the large-scale photospheric velocities. The case in point here is the velocities between 100 and 200 m s^{-1}, and 150 m s^{-1} may be taken as the mean value, which when projected onto the line of sight gives 110 m s^{-1}.

The total error in identifying line-of-sight velocities associated with supergranules, with the instrumental noise taken into account, will be 215 m s^{-1} (the square root of the sum of squares of all the above-listed errors). Because a change in the contribution from vertical motions to the projection onto the line of sight, with a displacement with respect to the centre of the solar disk, is roughly compensated by a change in the contribution from horizontal motions, this value can be extended to the entire area under consideration. From the aforesaid it follows that this value is the upper limit of the r.m.s. error.

References

Anzer, U. (1984) In: M. J. Hagyard (ed.), *Measurements of Solar Magnetic Fields*, NASA Conf. Publ. **2374**, 101.
Arter, W., Galloway, D. J., and Proctor, M. R. E. (1983) In: J. O. Stenflo (ed.), *Solar and Stellar Magnetic Fields*, IAU Symp. 102, p. 243.
Brandt, P. N., Scharmer, G.B., Ferguson, S., Shine, R. A., Tarbell, T. D., and Title, A. M. (1988) *Nature* **335**, 238.
Brandt, P. N., Ferguson, S., Scharmer, G. B., Shine, R. A., Tarbell, T. D., and Topka, K. (1991) *Astron. Astrophys.* **241**, 219.
Cartledge, N. P. and Priest, E. R. (1994) In: M. Heyn, W. Kernbickler and H. Biernat (eds.), *Current Topics in Astrophysical and Fusion Research*, Inst. Theor. Phys., Graz, p. 30.
Demoulin, P. and Priest, E. R. (1993) *Solar Phys.* **155**, 283.
Drobyshevski, E. M. and Yuferev, V. S. (1974) *J. Fluid Mech.* **65**, 38.
Foukal, P. (1971) *Solar Phys.* **19**, 59.
Garcia de la Rosa, J. I. (1983) *Solar Phys.* **89**, 51.
Gary, G. A., Moor, R. L., Hagyard, M. J., and Haish, B. M. (1987) *Astrophys. J.* **314**, 782.
Gary, G. A. and Hagyard, M. J. (1990) *Solar Phys.* **126**, 21.
Grigoryev, V. M., Kobanov, N. I., Osak, B. F., Selivanov, V. L., and Stepanov, V. E. (1985) In: M. J. Hagyard (ed.), *Measurements of Solar Vector Magnetic Fields*, NASA Conf. Publ. **2374**, 231.
Hirayama, T. (1985) *Solar Phys.* **100**, 415.
Hood, A. W. and Priest, E. R. (1979) *Solar Phys.* **64**, 303.
Hundhausen, J. R. and Low, B. (1994) *Astrophys. J.* **429**, 876.
Ioshpa, B. A. and Kulikova, E. H. (1995) *Soviet. Astron.* **72**, 932.
Kartashova, L. G. (1979) *Izv. Krymsk. Astrofiz. Observ.* **59**, 73.
Kippenhahn, R. and Schluter, A. (1957) *Z. Astrophys.* **243**, 36.
Kobanov, N. I. (1985) *Astron. Astrophys.* **143**, 99.
Kuperus, M. and Raadu, M. A. (1974) *Astron. Astrophys.* **23**, 189.
Low, B. C. (1993) *Astrophys. J.* **409**, 798.
Malherbe, J. M., Schmieder, B., and Mein, P. (1981) *Astron. Astrophys.* **102**, 124.
Martin, S. F., Bilimora, R., and Tracadas, P. W. (1994) In: R. J. Rutten and C. J. Schrijver (eds.), *Solar Surface Magnetism*, Springer, New York, p. 303.
Martin, S. F. and Echols, C. R. (1994) In: R. J. Rutten and C. J. Schrijver (eds.), *Solar Surface Magnetism*, Springer, New York, p. 339.
Plocienia, S. and Rompolt, B. (1973) *Solar Phys.* **29**, 399.
Priest, E. R., Hood, A. W., and Anzer, U. (1989) *Astrophys. J.* **344**, 1010.
Priest, E. R., Van Ballegooijen, A. A., and MacKay, D. H. (1996) *Astrophys. J.* **460**, 530.
Rimmele, T. and Schroter, E. H. (1989) *Astron. Astrophys.* **221**, 137.
Rust, P. M. and Kumar, A. (1994) *Solar Phys.* **155**, 69.
Sykora, J. (1968) *Bull. Astron. Inst. Czechosl.* **19**, 37.
Title, A. M., Tarbell, T. D., and the SOUP Team (1986) *Theoretical Problems in High Resolution Solar Physics*, NASA Conference Publ. **2483**, p. 55.
Title, A. M., Tarbell, T. D., Topka, K. P., Ferguson, S. H, Shine, R. A., and the SOUP Team (1989) *Astrophys. J.* **336**, 475.
Tsap, T. T. (1964) *Izv. Krymsk. Astrofiz. Observ.* **31**, 20.
Van Ballegooijen, A. A. and Martens, P. (1989) *Astrophys. J.* **343**, 971.
Van Ballegooijen, A. A. and Martens, P. (1990) *Astrophys. J.* **361**, 283.